

Transfer to Distant Retrograde Orbits Using Manifold Theory

Jacob Demeyer*

Delft University of Technology, 2629 HS Delft, The Netherlands
and

Pini Gurfil†

Technion—Israel Institute of Technology, 32000 Haifa, Israel

DOI: 10.2514/1.24960

The purpose of this work is to develop transfer trajectories from Earth to prespecified distant retrograde orbits in the sun–Earth planar circular restricted three-body problem by using orbits about the collinear equilibrium point L_1 . More specifically, we examine whether it is possible to use the hyperbolic network associated with the horizontal Lyapunov orbits around L_1 to find transfer trajectories to a wide range of distant retrograde orbits that are more energy-efficient and/or time-efficient compared with standard impulsive maneuvers. We point out how to apply manifold theory in the transfer-trajectory design process and show that for a certain class of distant retrograde orbits, the dynamic systems approach reveals the availability of transfer trajectories having reduced energy requirements or considerably reduced transfer times.

I. Introduction

A DISTANT retrograde orbit (DRO) is a stable orbit found in the circular restricted three-body problem (CRTBP). A spacecraft following a DRO flies around the primary mass, but in formation with the secondary mass, such that the orbits seem quasi elliptical around the latter object. Usually, orbits referred to as DROs have a characteristic dimension (semiminor axis) that is larger than the Earth– L_1 distance. In most works, DRO refers to orbits found in the sun–Earth CRTBP. They were first mentioned in the work of Hénon [1], studying Hill’s modification of the CRTBP. In that paper, the DROs are classified as the f family.

The motivation for studying DROs stems from their unique characteristics. These include the possibility to avoid near–Earth phenomena such as the magnetic and radiation fields and the possibility to keep the distance between the spacecraft and the Earth below a certain predefined value. These features are useful for certain astrophysical applications such as spaceborne optical telescopes and radio imaging of the sun.[‡] Another possible application is to use a formation of three or more vehicles on a DRO, providing a warning system for geomagnetic storms.

The transfer to a DRO can be accomplished in several ways. Transfers can use impulsive or finite burn propulsion. Optimal solutions can be found using direct or indirect optimization [2]. A number of works discussed indirect optimization of impulsive low–Earth–orbit (LEO)–to–DRO transfer trajectories using primer vector theory and indirect optimization of low–thrust LEO–to–DRO transfer trajectories using optimal control theory (based on the Pontryagin maximum principle) [3,4].

Some previously developed impulsive transfer trajectories are those categorized by Ocampo and Rosborough [5] as class A1 and class A2 transfers. In that work, transfer orbits were constructed using the continuation toward Earth of horizontal Lyapunov orbits (HLOs). These continued orbits are often called Earth–return orbits

(EROs), classified as the c family in Hénon’s work [1]. A transfer trajectory to a DRO is a slightly adapted half-cycle path of an (unstable) ERO. The transfer time to a representative DRO (semiminor axis of 5×10^6 km) using Ocampo’s method is approximately 230 days. The main disadvantage of this method is that only a certain range of DROs can be reached if only two impulses are allowed (the minor axes of these DROs lie between 4×10^6 and 20×10^6 km). This is because an ERO must approach the Earth close enough such that the trajectory can depart tangentially from some given LEO.

In this paper, we shall develop a transfer concept that extends the previously mentioned method, referred to as the *classical transfer* from this point on. The main goal is to extend the range of accessible DROs using a systematic approach and to achieve lower ΔV and/or shorter travel times. The key to this extension is the application of dynamic systems theory. More specifically, the dynamics around the collinear libration points, which are known to be hyperbolic, guaranteeing the existence of stable and unstable manifolds, will lead to a method for circumventing some of the restrictions of the classical transfer. It should be mentioned that this work will be restricted to impulsive transfers. Trajectory optimization will be performed using a direct-shooting optimization scheme.

The development of our *extended transfer* consists of the following steps. We first introduce the most important building blocks to be used for the design of the transfer trajectories. These include a description of the model for the CRTBP; a discussion of DROs, EROs, and HLOs; an introduction to manifold theory; and a definition of the transit orbits. We then give a brief description of the classical transfer concept and the required numerical techniques. This will enable us to introduce the extended transfer as a continuation of the classical transfer. By using numerical methods analogous to those used for the optimization of the classical transfer, we calculate ΔV values and travel times for a set of reachable DROs. Finally, we briefly discuss an alternative way to use manifolds in LEO–to–DRO transfer-trajectory design for a range of large DROs, including some preliminary ΔV and travel-time calculations.

II. Building Blocks for the Design of Transfer Trajectories

Before starting with the design of the transfer trajectories, we will briefly introduce the CRTBP model, discuss some of the different

Received 4 May 2006; accepted for publication 2 April 2007. Copyright © 2007 by the authors. Published by the American Institute of Aeronautics and Astronautics, Inc., with permission. Copies of this paper may be made for personal or internal use, on condition that the copier pay the \$10.00 per-copy fee to the Copyright Clearance Center, Inc., 222 Rosewood Drive, Danvers, MA 01923; include the code 0731-5090/07 \$10.00 in correspondence with the CCC.

*Graduate Student, Department of Astrodynamics and Satellite Systems, Faculty of Aerospace Engineering; J.R.C.Demeyer@student.tudelft.nl.

†Senior Lecturer, Faculty of Aerospace Engineering; pgurfil@technion.ac.il. Associate Fellow AIAA.

[‡]Data available online at <http://sira.gsfc.nasa.gov/> [retrieved 2 January 2006].

periodic orbits that will be used in this work, give a brief introduction to manifold theory, and define the transit orbits.

A. Circular Restricted Three-Body Problem

The dynamic model used in this work is the planar circular restricted three-body problem (CRTBP). Although DROs and EROs can have velocity components in a direction perpendicular to the ecliptic, we will only study planar motion. On one hand, this will keep the problem relatively simple. On the other hand, we expect that results for the planar motion are easily extendable to the case of motion in three dimensions (one reason for having out-of-plane velocity components for the final orbit, the DRO, is to avoid eclipse periods; another reason is to reduce the effect of the zodiacal dust cloud [6]).

Furthermore, it is assumed that the two main bodies (in this case, the sun and the Earth) are in circular orbits around their common barycenter and that the mass of the third body (the satellite) is negligible with respect to the masses of the two main bodies.

The dynamics are modeled using a rotating frame centered at the Earth. The x axis is directed from the origin in a direction away from m_1 , the primary, and the y axis points along the velocity vector of m_2 , the secondary. The unit of length is chosen to be the distance between the sun and the Earth. The unit of time is $1/\omega$, where ω is the constant angular velocity with which the frame rotates about the third, perpendicular, axis. The dimensionless planar equations of motion for the CRTBP are given by [7]

$$\begin{aligned} \ddot{x} - 2\dot{y} &= x + 1 - \mu - \frac{1-\mu}{r_1^3}(x+1) - \frac{\mu}{r_2^3}x \\ \ddot{y} + 2\dot{x} &= y - \frac{1-\mu}{r_1^3}y - \frac{\mu}{r_2^3}y \quad \ddot{z} = -\frac{1-\mu}{r_1^3}z - \frac{\mu}{r_2^3}z \end{aligned} \quad (1)$$

with r_1 and r_2 defined as

$$r_1^2 = (x+1)^2 + y^2 + z^2 \quad r_2^2 = x^2 + y^2 + z^2 \quad (2)$$

and the mass ratio μ defined as

$$\mu = \frac{m_2}{m_1 + m_2} \quad (3)$$

where it is assumed that m_2 is the combined Earth–moon mass. The data used for the calculations are taken from Ocampo and Rosborough [5] to make the comparison valid and are summarized in Table 1.

The model described earlier is used for a variety of calculations in the subsequent discussion. One of the applications is the numerical search for EROs, DROs, and HLOs (Sec. II.B). The second major use of the model is for the calculation of manifolds (Sec. II.C).

B. Periodic Orbits in the CRTBP

The most important class of CRTBP orbits needed for this work is the linearly stable planar DRO family. A spacecraft following a DRO flies around the primary mass, but in formation with the secondary mass, such that the orbits seem quasi-elliptic around the latter object. Usually, orbits referred to as DROs have a characteristic dimension that is larger than the Earth– L_1 distance. In most works, DRO refers to orbits found in the sun–Earth CRTBP. Figure 1 shows some DROs calculated in the CRTBP. The three dots in the middle of the plot are,

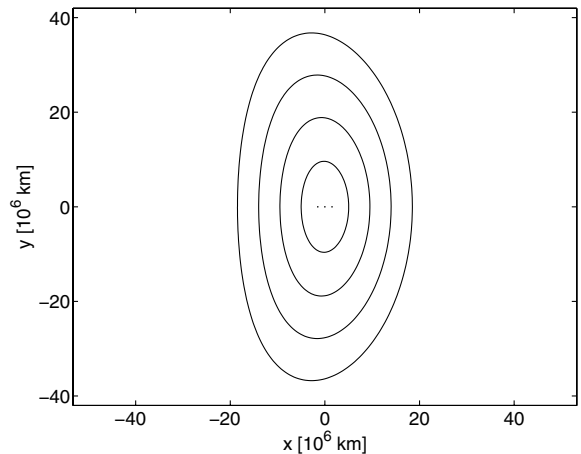


Fig. 1 Representative distant retrograde orbits; the three dots in the middle of the plot are L_1 , the Earth, and L_2 (from left to right).

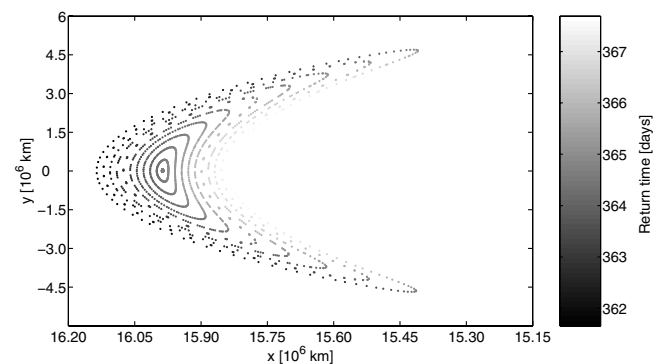


Fig. 2 Phase-space structure around a 16×10^6 km DRO illustrated using a Poincaré section at $x = 0$ and $dx/dt > 0$; every trajectory on this section has the same Jacobi constant, the fixed point represents the DRO, the closed curves around it indicate the presence of invariant tori, and the gray scale indicates return times in days.

from left to right, the first Lagrange point L_1 , the Earth, and the second Lagrange point L_2 .

The dynamics of DROs under the presence of perturbations can be foreseen using a Poincaré section of the phase space around these orbits. Figure 2 shows the phase-space structure around a DRO with a semiminor axis of 16×10^6 km. As can be seen, perturbations will cause a vehicle to move on invariant Kolmogorov–Arnold–Moser tori [8] close to the DRO. The grayscale indicates that return times (in days) of these perturbed orbits are comparable with the DRO periods. In practice, this means that natural perturbations and/or small deviations from the calculated impulsive maneuvers are feasible.

In addition to DROs, some other periodic orbits will be important for the development of the transfer trajectories: EROs and associated HLOs. EROs are a class of unstable periodic orbits in the CRTBP, first categorized by Hénon [1] as the a family. They periodically approach and leave a close neighborhood of the Earth. As illustrated in Fig. 3, there is a wide range of EROs (including a symmetric family of EROs centered at L_2 , which is not shown), some of which can be continued toward the Lagrange point L_1 , where they become simple quasi-elliptical HLOs.

Table 1 Summary of the circular restricted three-body problem model parameters

Parameter	Symbol	Value	Units
Sun mass	m_s or m_1	1.9891×10^{30}	kg
Combined Earth–moon mass	$m_e + m_m$ or m_2	6.04773×10^{24}	kg
Sun–Earth distance	AU	149.598×10^9	m
Sun–Earth angular velocity	ω	1.9910×10^{-7}	$1/s^2$
CRTBP mass ratio	μ	$3.04042389 \times 10^{-6}$	—

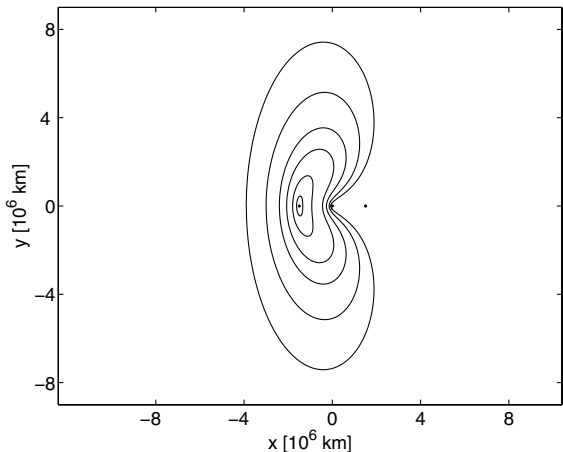


Fig. 3 Examples of EROs and HLOs around L_1 ; dots in the figures represent L_1 , the Earth, and L_2 (from left to right); small, nearly elliptical, orbits are HLOs; larger orbits are the so-called EROs.

C. Manifold Theory

As shown in several papers [9–11], the collinear libration points in the CRTBP are of the center \times center \times saddle type in three dimensions and of the center \times saddle type in two dimensions. An important consequence of this center \times saddle behavior is the existence of stable and unstable manifolds. These structures can be interpreted as a higher-dimensional equivalent of the stable and unstable directions associated with a saddle point. This means that any particle moving on a stable manifold of an orbit will asymptotically approach that orbit without providing external energy [12]. Any particle moving on the unstable manifold of the orbit will asymptotically leave the orbit.

Figure 4 shows a branch of a stable manifold in the direction of the Earth and the branch of an unstable manifold in the direction of the sun. The manifolds shown in the plot are associated with an HLO having a semiminor axis of 90×10^3 km in the sun–Earth CRTBP.

There are many applications of manifold theory found in the literature. Some works discuss how connections of the stable and unstable manifolds of different neighboring three-body systems can be used to transfer object from one system to another with negligible fuel consumption. One such application is the Petit Grand Tour of the moons of Jupiter [13], showing the feasibility of a low-energy manifold-to-manifold trajectory that passes by the major moons of Jupiter. However, for what follows, the most important classes of applications are those in which the stable manifolds found in the sun–Earth system are used for the transfer from Earth to the HLOs or halo orbits (three-dimensional equivalents of the HLOs) [12,14]. The stable manifolds associated with L_1 -centered HLOs and EROs approach the Earth very closely, which makes them attractive for

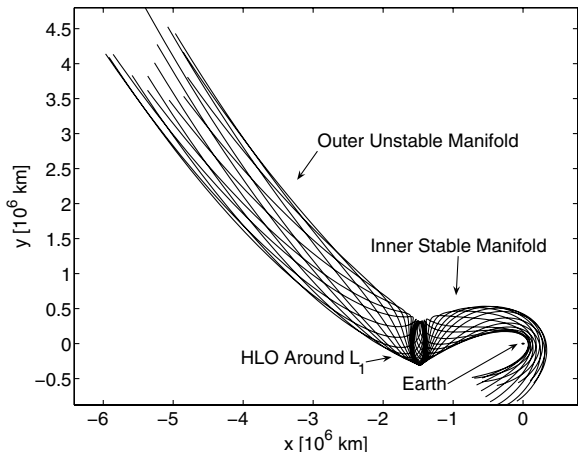


Fig. 4 Stable and unstable manifolds around L_1 ; the HLO has a semiminor axis of 90×10^3 km.

efficient Earth-to-HLO or Earth-to-halo transfers. In Sec. IV, we show how this property can be applied to the LEO-to-DRO transfer.

As a final remark, it should be noted that similar manifolds can be found for HLOs around L_2 . However, this work will concentrate on trajectory design using the hyperbolic network around L_1 only.

D. Transit Orbits

When connecting stable and unstable manifolds during trajectory design, it is impractical to assume that the spacecraft asymptotically approaches or leaves an HLO. In all practical cases, one would rather use a finite time transit orbit. A brief discussion on this topic will be given later; more details can be found elsewhere [15,16].

In position space, transit orbits always lie within the boundaries of the stable and the unstable manifolds. The conditions imposed on the initial velocities of an orbit to render it a transit orbit can be formulated in terms of *velocity wedges* [15]. Three such wedges are shown in Fig. 5. Orbits with velocity interior to the wedge are transit orbits; orbits with velocity on the boundary of the wedge are asymptotic, coinciding with the manifold curves; and orbits with velocity outside the wedge are nontransit. Alternatively, a spacecraft will follow a transit orbit if it starts with initial conditions that 1) lie within the boundaries of the stable manifold (in the x - y space) and 2) are contained within the velocity wedge (in the \dot{x} - \dot{y} space).

In Fig. 6, different transit orbits are shown. They are calculated by integrating the CRTBP starting at a point with initial velocities that are slightly different than a point lying on the stable manifold close to the Earth (inside the velocity wedges). The continuous lines give the boundaries (in x - y space) of the unstable manifold. As can be seen, all possible transit orbits always remain within those boundaries, which makes the concept of manifold tubes and associated transit orbits a powerful tool for trajectory design.

III. Classical Transfer Concept

The classical transfer concept [5] uses the previously mentioned ERO (Fig. 3), which can always be chosen so as to intersect tangentially with the target DRO on the x axis. Thus, the last impulsive maneuver is easily chosen to be tangential to the velocity vector.

The initial (parking) orbit is assumed to be a 200-km prograde LEO with its orbital plane coinciding with the x - y plane. Because the LEO and the ERO usually do not intersect tangentially, one could think of a transfer concept in which a two-body elliptic or hyperbolic orbit connects the LEO with the ERO, resulting in a three-impulse transfer.

A second option is to use a differential corrector to adapt an estimated transfer trajectory (the ERO) such that it does intersect tangentially with the assumed parking orbit. For most of the

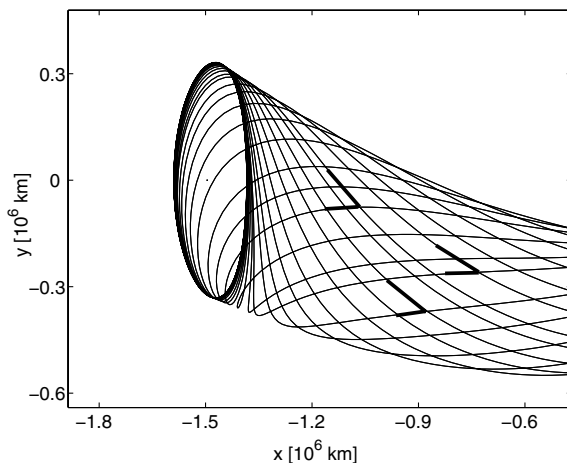
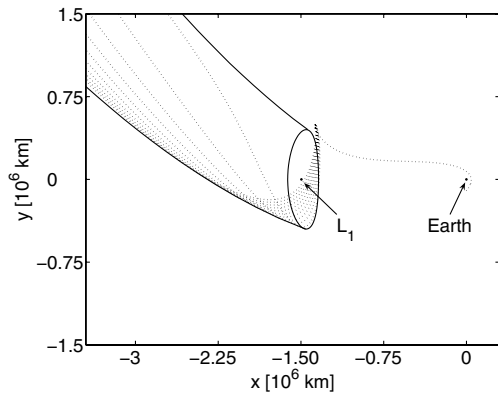
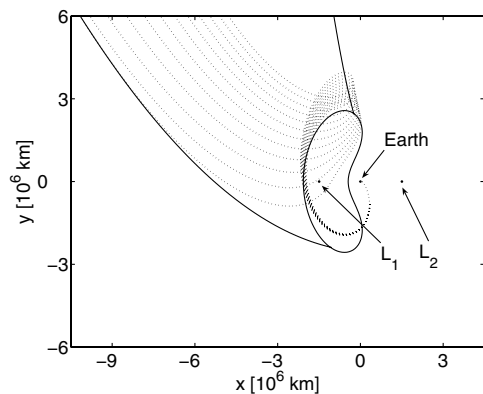


Fig. 5 Velocity wedges and a manifold of an HLO; orbits with velocity interior to the wedge are transit orbits, orbits with velocity on the boundary of the wedge are asymptotic, and orbits with velocity outside the wedge are nontransit.



a) Transit orbits, HLO with semiminor axis of 120×10^6 km



b) Transit orbits, HLO with semiminor axis of 570×10^6 km

Fig. 6 Transit orbits (dotted lines); boundaries of the unstable manifold are plotted as continuous lines departing the HLO; note that the scales of both figures are different.

calculations in this work, this option, which will result in a two-impulse transfer trajectory, is preferred. This differential corrector approach will be clarified shortly.

The transfer trajectories will be obtained by using a direct-shooting optimization scheme. The quantity to be minimized is the sum of the N ΔV values of the impulsive maneuvers. As such, the objective function F can be written as

$$F = \Delta V_{\text{tot}} = \sum_{i=1}^N \Delta V_i \quad (4)$$

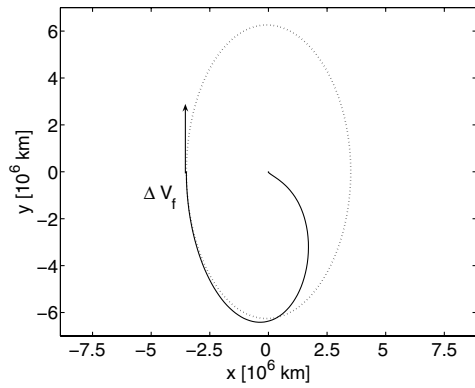
Imposing tangentiality of the transfer trajectory to the parking orbit (at time t_0) and to the DRO target orbit (at time t_f) is done by adding a set of equality constraints \mathbf{c} to the optimization scheme. These can be written as

$$\mathbf{c}(t_i) = \begin{cases} c_r & = r(t_i) - R_i(\theta_i) = 0 \\ c_{\tan} & = \tan^{-1}[v_x(t_i)/u_x(t_i)] - \tan^{-1}[V_x(\theta_i)/U_x(\theta_i)] = 0 \end{cases} \quad (5)$$

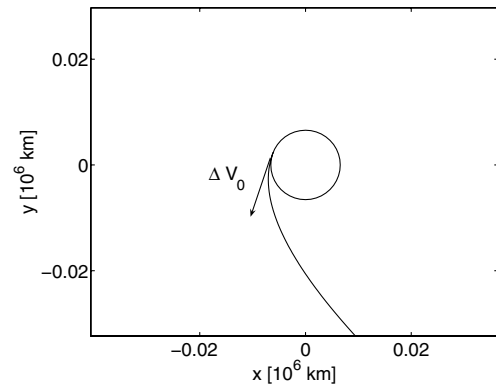
where $r(t_i)$, $u(t_i)$, and $v(t_i)$ are the radius (distance to the Earth) and the velocity components in the x and y directions of the transfer trajectory at time t_i , respectively. R_i , U_i , and V_i are Chebyshev polynomial expressions [17] for the radius and the velocity components in the x and y directions for the LEO ($i = 0$) or for the DRO ($i = f$) as a function of the polar angle θ . These constraints are imposed at the initial and final times t_0 and t_f , respectively.

Finally, the parameter vector for the two-impulse transfer is defined as

$$\mathbf{X} = [\theta_f \ \Delta V_f \ t_f]^T \quad (6)$$



a) Transfer from LEO to DRO



b) Transfer from LEO to DRO: near-Earth detail

Fig. 7 Transfer from LEO to DRO using the method by Ocampo [5], the classical transfer: a) DRO (dashed line) and ERO-like (solid line) transfer trajectory and b) detail of the trajectory close to the Earth; the circular orbit is the initial LEO parking orbit.

where θ_f is the polar angle at t_f and ΔV_f is the size of the tangential impulsive maneuver at t_f . Assuming that $t_0 = 0$, these parameters uniquely specify the particular transfer trajectory.

With the half-cycle path of an appropriate ERO as the initial estimate, the optimization scheme converges to two-impulse solutions similar to those given in Fig. 7. Resulting travel times and ΔV values for transfer to DROs with semiminor axes from 4 – 20×10^6 km vary almost linearly from 215–250 days and from 3290–4000 m/s, respectively. Comparable values can be found in several works by Ocampo [4,5] (230 days and 3372 m/s for the transfer to a DRO with a semiminor axis of 5×10^6 km).

IV. Extending Transfer Design Using Manifold Theory

In this section, we will show how manifold theory can be used to efficiently calculate transfer trajectories to a range of small DROs. Although the classical method concentrated on DROs easily accessible using ERO-like trajectories, we will shift the focus to DROs with semiminor axes smaller than 4×10^6 km, which could be very useful for deep-space science missions.

As seen in Fig. 3, EROs can be used as the initial estimates of transfer trajectories to a wide range of DROs. However, smaller DROs would require smaller EROs. Reducing the semiminor axis of the target DRO below 4×10^6 km will necessitate using an HLO, but not an ERO, as a candidate transfer trajectory. Thus, the traditional use of the ERO half-cycle path as an initial estimate for the transfer trajectory can no longer be used.

The solution to this problem, termed the *extended method*, is to use a trajectory that lies on the stable manifold of an appropriate HLO (i.e., an HLO that crosses the x axis where the target DRO crosses the x axis). This approach considers the manifolds to be a natural extension of the orbit. In other words, one can say that any object on a stable manifold of some orbit is already on that orbit. With this concept in mind, using a trajectory on the stable manifold as a

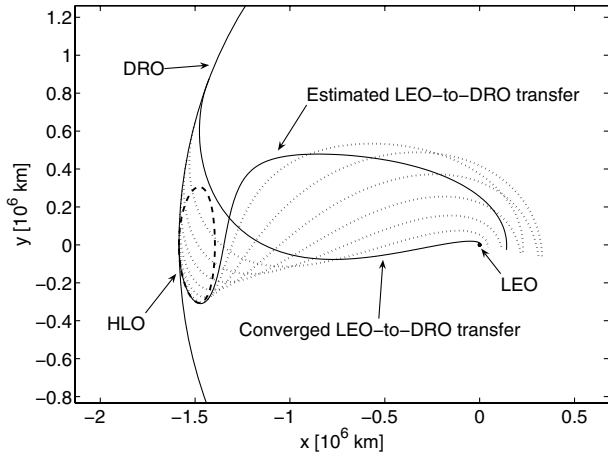


Fig. 8 Initial manifold trajectory guess converges onto an optimal transfer trajectory.

transfer-trajectory estimate constitutes a natural extension of the classical method.

We will first apply the extended method to a target DRO with a semiminor axis of 1.65×10^6 km. The initial guess \mathbf{X}_0 , describing the transfer-trajectory initial estimate, was calculated using Eqs. (4–6). This transfer trajectory is shown in Fig. 8. It is clearly seen that this trajectory lies on the inner stable manifold of the selected HLO (see Fig. 4). The dotted lines in Fig. 8 show that the optimization scheme converges onto the optimal trajectory under the tangentiality constraints. The bottom solid line shows the resulting optimal transfer trajectory.

Figure 9 shows several transfer trajectories for a number of small DROs. In this figure, it is easy to see that the manifoldlike transfer trajectories for the very small DROs (as shown in Fig. 8) tend toward ERO-like trajectories when increasing the size of the target DROs, thus complying with the classical transfer.

Figure 10 summarizes the results obtained from the optimization in terms of required ΔV and travel time for both the classical (semiminor axis larger than 4×10^6 km) and the extended transfer (semiminor axis smaller than 4×10^6 km). The continuity-type relationship between the classical and extended transfer becomes evident. Table 2 provides some numerical data for a representative set of small DROs (semiminor axis smaller than 4×10^6 km).

An important observation is that with the extended transfer, there is a DRO for which the total transfer ΔV is minimal. This DRO has a semiminor axis of approximately 2.75×10^6 km and a total required ΔV of 3277 m/s. The travel time to this DRO is approximately 165 days. Furthermore, Fig. 10 reveals that the travel time can be reduced dramatically if the DRO's semiminor axis becomes smaller. However, decreasing the size of the target DRO below a semiminor axis of 1.55×10^6 km incurs an exponential increase in the required

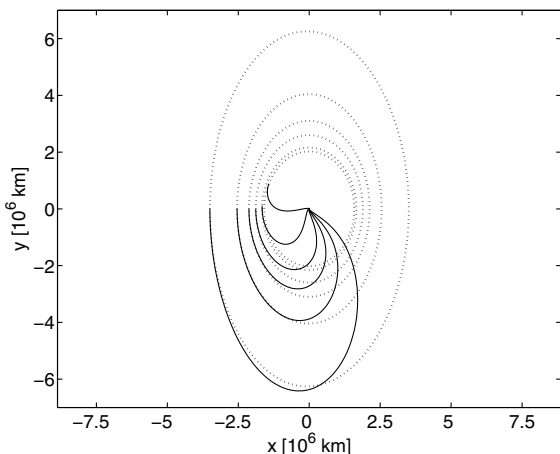


Fig. 9 Optimal transfer trajectories to selected small DROs.

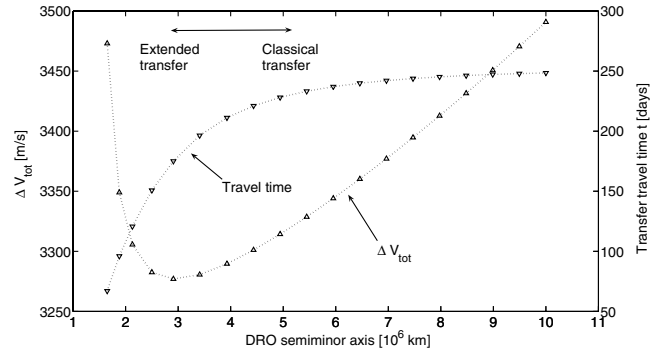


Fig. 10 Required ΔV and travel time as a function of the target DRO semiminor axis. Combined classical transfer (right side) and extended transfer (left side).

ΔV . The reason for this is the location of the L_1 Lagrange point at $x = -1.5 \times 10^6$ km (in an Earth-centered reference frame).

Figure 10 can also be used for comparing the classical and extended transfers. First, the extended transfer reveals the possibility of reducing travel times dramatically, compared with the classical transfer. More important, the extended transfer discloses a range of DROs (semiminor axes between 2.75×10^6 and 4×10^6 km) that require a *smaller* ΔV than the classical transfer. Thus, a new realm of possibilities is opened to the mission designer, who can now choose a mission orbit from a wide range of DRO sizes.

Finally, in the case of a three-impulse transfer, the optimization parameter vector is defined as

$$\mathbf{X} = [\theta_f \ \Delta V_1 \ \Delta V_f \ t_1 \ t_f]^T \quad (7)$$

where ΔV_1 is the second (intermediate) impulsive maneuver at time t_1 . Assuming that $t_0 = 0$, these parameters uniquely specify a particular transfer trajectory. Resulting ΔV values and travel times for the three- and two-impulse transfers differ by only a few tenths of a percent. However, the range of reachable DROs is extended toward even smaller semiminor axes. A major disadvantage of the very small DROs is an exponential increase in ΔV , as indicated earlier.

V. Transfer to Large Distant Retrograde Orbits

Thus far, the extended method has focused on DROs with semiminor axes that are smaller than those within reach of the classical method. However, one could also think of applying dynamic systems theory for transferring to DROs with semiminor axes that are larger than those reachable using the classical method. In the following discussion, the feasibility of this idea will be examined.

To begin, it is interesting to look at the behavior of the unstable manifolds departing the HLOs or small EROs. As can be seen in Fig. 4, making use of these manifolds might indeed provide opportunities to reach DROs with very large semiminor axes.

A transit orbit, as described in Sec. II.D, would make the object approach the libration-point neighborhood on the stable manifold and subsequently direct the object away from the libration-point neighborhood inside the unstable manifold tube, without the need to provide extra energy. Figure 11 shows an example of such an Earth-to-DRO transfer trajectory.

As can be seen, the final impulsive maneuver, required to transfer the satellite from the unstable manifold to the DRO, will generally

Table 2 Summary of transfer-trajectory characteristics for selected DROs

DRO semiminor axis, km	Total ΔV , m/s	Travel time, days
1.65×10^6	3473	67
1.88×10^6	3349	96
2.91×10^6	3277	175
3.93×10^6	3289	211

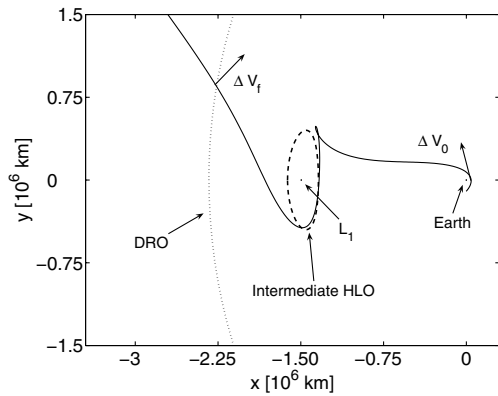


Fig. 11 Transfer from LEO to DRO using the transit orbit approach.

not be tangential to the target velocity vector on the DRO. In terms of required ΔV for this maneuver, this is not an ideal situation. However, the different manifold curves and the wide range of useful HLOs (from which the manifolds are calculated) yield some flexibility for optimizing the transfer. Furthermore, it is expected that by avoiding the ERO-like transfer trajectories as in the classical transfer, a considerable reduction of the travel time can be achieved, possibly at the expense of a slightly higher ΔV .

In what follows, the goal is to estimate how attractive this alternative transfer concept is in terms of the required ΔV and/or travel time. First, we will show the relation between the previously developed transfer methods and the current method. Second, it will be explained how a coarse random optimization scheme (similar to Monte Carlo optimization) was applied to make estimates of feasible trajectories. Finally, it will be shown that the multitude of possible transit orbits will increase the tradeoff flexibility (enabling a tradeoff between required ΔV and travel time) in the design of the trajectory.

Calculating the second impulsive maneuver ΔV_f that would be required for different target DROs using a trajectory on the unstable manifold of differently sized intermediate HLOs results in relations such as those shown in Fig. 12. In this figure, ΔV_f is calculated as a function of the semiminor axis of the intermediate HLO for a target DRO with a semiminor axis of 4×10^6 km. Examining the slope of the curve in this figure makes it evident that even lower ΔV values should be achievable for larger semiminor axes of the HLOs (the extreme right in Fig. 12). It will thus be assumed that ΔV_f will approach the value found in Sec. III when the intermediate HLO or ERO further approaches the DRO. This would reduce the current transfer design methodology to the classical transfer concept. To understand this, one can examine Figs. 9 and 11: Once the HLO or ERO and the DRO osculate, the current transfer concept reduces to the classical transfer. Consequently, the current transfer design can be understood as a generalized approach, of which the classical method is a special case.

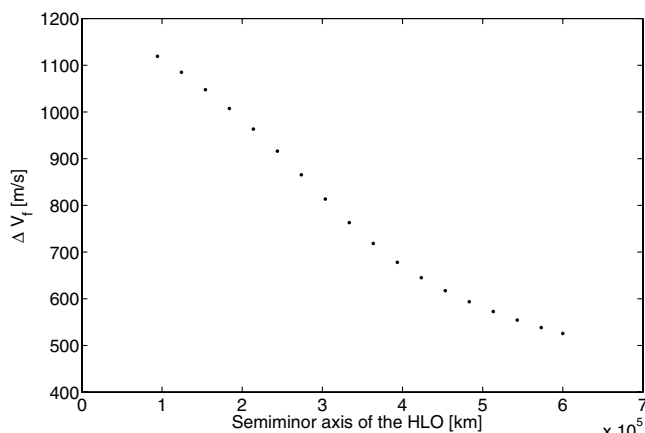


Fig. 12 Required ΔV_f for the transfer to a DRO with semiminor axis 4×10^6 km for different intermediate HLOs or EROs.

Table 3 Summary of transfer-trajectory characteristics for large DROs

DRO semiminor axis, km	Total ΔV , m/s	Travel time, days
5×10^6	6202	23
5×10^6	3998	59
5×10^6	3478	151
15×10^6	8200	58
15×10^6	4875	119
30×10^6	9626	99
30×10^6	7513	135

In estimating ΔV_f , it was assumed that the object was already on the unstable manifold of some HLO or ERO. It should be realized, however, that this situation is not practically achievable, because a vehicle on a stable manifold will always approach the orbit (ERO or HLO) asymptotically. The solution to this problem is to use the so-called transit orbit, which does not lie on the stable or unstable manifolds but is enclosed by those manifolds (cf. Sec. II.D). Realizing that there are a myriad of possible transit orbits, it is obvious that there is a certain flexibility in choosing the desired combination of required ΔV and travel time. By carrying out a simplified random (Monte Carlo) optimization scheme with a parameter vector,

$$\mathbf{X} = [\theta_0 \ \Delta V_0]^T \quad (8)$$

where ΔV_0 is the first impulsive maneuver applied in the initial parking LEO at a polar angle θ_0 , a number of feasible solutions can be found for different target DROs. The possible values for the parameters \mathbf{X} were kept within reasonable bounds derived from earlier trajectory calculations. Assuming two objective functions, $F_1 = \Delta V_{\text{tot}}$ and $F_2 = t_f$, these calculations result in a Pareto-optimal set for each target DRO. Some values for ΔV and t_f contained in that set are given in Table 3.

Because of the nontangential impulsive maneuver required for the current concept (and considering the trend in Fig. 12), it can be safely assumed that the transfer concept discussed in earlier sections will always be fuel-optimal.

The ΔV and travel time required to reach DROs with semiminor axes of 5×10^6 and 30×10^6 km using the classical transfer can be calculated to be 3315 m/s and 230 days and 4700 m/s and 250 days, respectively. Similar values for intermediate-sized DROs can be calculated using a linear interpolation.

With this in mind, the continuous curve showing the relation between the semiminor axis of the target DRO and the total required ΔV for both the classical (semiminor axis larger than 4×10^6 km) and the extended (semiminor axis smaller than 4×10^6 km) transfers is plotted as a bold lower boundary in Fig. 13 (travel times for this range of transfer trajectories is not included in this figure). Note the correspondence between the ΔV curve in Fig. 10 and the leftmost part of the bold line in Fig. 13. Completing this figure is done using the ΔV and travel-time data (Pareto-optimal set) obtained from the

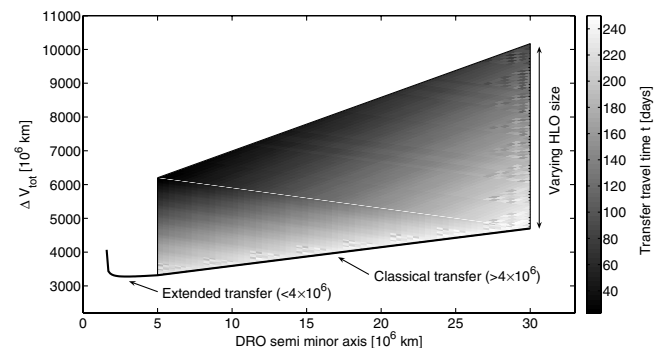


Fig. 13 Summary of ΔV and travel-time estimates for the classical and extended transfer concepts (bold line) and the current method, used for transferring to large DROs.

Monte Carlo optimization. A number of these (exact) values for different target DROs are used to make the interpolation, shown as a gray area in Fig. 13.

Figure 13 can be used to make a first estimate of the ΔV and travel times required to reach different target DROs using varying intermediate HLO/EROs sizes. The plot can be straightforwardly extended toward even larger DROs; however, the increasing travel times and, more important, required ΔV , might render these DROs less attractive.

The most interesting conclusion that can be drawn from the preceding calculations is the dramatic decrease in travel time for a wide range of DROs. For example, to travel to a DRO with a semiminor axis of 5×10^6 km, which would require a ΔV of 3315 m/s and a travel time of 230 days using the classical method [5], one could consider a 5% ΔV increase (from 3315 to 3478 m/s) to get a 35% travel-time reduction (from 230 to 150 days) or a 20% ΔV increase (from 3315 to 3998 m/s) to get a 75% travel-time reduction (from 230 to 59 days). Similar estimates can be made using Fig. 13.

VI. Conclusions

In this paper, we applied some tools of dynamic systems theory to the LEO-to-DRO transfer problem. The goal was to extend the range of accessible DROs using a systematic approach and to achieve lower ΔV values and/or travel times. The dynamic systems approach was shown to be more rigorous than direct numerical methods.

We conclude that the dynamic systems approach can provide transfer orbits to a wider range of DROs (e.g., smaller DROs). Furthermore, this approach indicates the availability of transfer orbits that are more efficient in terms of ΔV budgets and/or travel times. For example, the optimization used for expanding the transfer to smaller DROs indicated that a certain range of DROs (semiminor axes around 2.75×10^6 km) required a minimum amount of ΔV at a substantially smaller travel time (around 160 days). Decreasing the DRO semiminor axis even further permits reducing the travel time at the expense of a slightly increased ΔV .

Finally, our analysis indicated the availability of transfer trajectories providing dramatically shorter travel times for a certain range of target DROs (semiminor axis larger than 5×10^6 km) at a cost of a slightly increased ΔV . We have shown that for a transfer to a DRO with a semiminor axis of 5×10^6 km, one could consider a 20% ΔV increase to get a 75% travel-time reduction compared with the classical transfer.

Acknowledgments

Support for this work was obtained through the Fonds Internationale Stages of the Delft University of Technology and through the financial advantages offered by the Student Exchange Program agreements between Technion—Israel Institute of Technology and Delft University of Technology. The authors are in debt of gratitude to Cesar Ocampo for making valuable and constructive comments. This research was performed during the internship of the first author in the Faculty of Aerospace Engineering at the Technion—Israel Institute of Technology.

References

- [1] Hénon, M., "Numerical Exploration of the Restricted Problem 5, Hill's Case: Periodic Orbits and Their Stability," *Astronomy and Astrophysics*, Vol. 1, Feb. 1969, pp. 223–238.
- [2] Betts, J., "Survey of Numerical Methods for Trajectory Optimization," *Journal of Guidance, Control, and Dynamics*, Vol. 21, No. 2, 1998, pp. 193–207.
- [3] Ocampo, C., and Rosborough, G., "Multiple-Spacecraft Orbit Transfer Problem: The No-Booster Case," *Journal of Guidance, Control, and Dynamics*, Vol. 22, No. 5, 1999, pp. 650–657.
- [4] Ocampo, C., "Trajectory Optimization for Distant Earth Satellites and Satellite Constellations," Ph.D. Thesis, Department of Aerospace Engineering Sciences, Univ. of Colorado, Boulder, CO, 1996, pp. 47–82; Chaps. 3–4.
- [5] Ocampo, C., and Rosborough, G., "Transfer Trajectories for Distant Retrograde Orbiters of the Earth," *Spaceflight Mechanics 1993*, Advances in the Astronautical Sciences, Vol. 82, Pt. 2, for American Astronautical Society by Univelt, San Diego, CA, 1993, pp. 1177–1200.
- [6] Gurl, P., and Kasdin, N. J., "Optimal Out-of-Ecliptic Trajectories for Space-Borne Observatories," *Journal of the Astronautical Sciences*, Vol. 49, No. 4, 2001, pp. 509–537.
- [7] Szebehely, V., *Theory of Orbits: The Restricted Problem of Three Bodies*, Academic Press, New York, 1967, pp. 7–22; Chap. 1.
- [8] Verhulst, F., *Nonlinear Differential Equations and Dynamical Systems*, Springer-Verlag, New York, 2000, pp. 243–245.
- [9] Gómez, G., Koon, W., Lo, M., Marsden, J., Masdemont, J., and Ross, S., "Connecting Orbits and Invariant Manifolds in the Spatial Restricted Three-Body Problem," *Nonlinearity*, Vol. 17, No. 5, 2004, pp. 1571–1606.
- [10] Jorba, A., and Masdemont, J., "Dynamics in the Center Manifold of the Collinear Points of the Restricted Three Body Problem," *Physica D*, Vol. 132, Nos. 1–2, 1999, pp. 189–213.
- [11] Simo, C., and Stuchi, T., "Central Stable/Unstable Manifolds and the Destruction of KAM Tori in the Planar Hill Problem," *Physica D*, Vol. 140, No. 1, 2000, pp. 1–32.
- [12] Gómez, G., Jorba, A., Masdemont, J., and Simó, C., "Study of the Transfer from the Earth to a Halo Orbit Around the Equilibrium Point L_1 ," *Celestial Mechanics and Dynamical Astronomy*, Vol. 56, No. 4, 1993, pp. 541–562.
- [13] Koon, W., Lo, M., Marsden, J., and Ross, S., "Constructing a Low Energy Transfer Between Jovian Moons," *Contemporary Mathematics*, edited by A. Chenciner, R. Cushman, C. Robinson, and Z. Xia, Vol. 292, American Mathematical Society, Providence, RI, 2002, p. 129.
- [14] Senent, J., Ocampo, C., and Capella, A., "Low-Thrust Variable-Specific-Impulse Transfers and Guidance to Unstable Periodic Orbits," *Journal of Guidance, Control, and Dynamics*, Vol. 28, No. 2, 2005, pp. 280–290.
- [15] Conley, C., "Low Energy Transit Orbits in the Restricted Three-Body Problem," *SIAM Journal on Applied Mathematics*, Vol. 16, No. 4, 1968, pp. 732–746.
- [16] Koon, W., Lo, M., Marsden, J., and Ross, S., "Heteroclinic Connections Between Periodic Orbits and Resonance Transitions in Celestial Mechanics," *Chaos*, Vol. 10, No. 2, 2000, pp. 427–469.
- [17] Ocampo, C., and Rosborough, G., "Optimal Low-Thrust Transfers Between a Class of Restricted Three-Body Trajectories," *Astrodynamics 1993*, Advances in the Astronautical Sciences, Vol. 85, Pt. 2, for American Astronautical Society by Univelt, San Diego, CA, 1994, pp. 1547–1566.